Hydrometallurgy 221 (2023) 106145

Contents lists available at ScienceDirect

Hydrometallurgy

journal homepage: www.elsevier.com/locate/hydromet

Biological extraction of Cu and Ni from printed circuit boards via redoxolysis with concomitant material characterization

Arevik Vardanyan [a,b,*], Narine Vardanyan [a], Stoyan Gaydardzhiev [b]

[a] SPC "Armbiotechnology" of National Academy of Sciences of Armenia, Gyurjyan 14, Yerevan 0056, Armenia
[b] GeMMe-Mineral Processing and Recycling, University of Liege, Allée de la Decouverte 9, Sart Tilman, Liege 4000, Belgium

ARTICLE INFO

Keywords:
Printed circuit boards (PCBs)
Biogenic ferric iron
Redoxolysis
Acidithiobacillus ferrooxidans 61
Scanning electron microscope (SEM)/energy dispersive spectroscopy (EDS)

ABSTRACT

Among the different types of secondary post-consumption wastes, *E*-wastes or waste electrical and electronic equipment represent the fastest growing and most problematic waste stream with printed circuit boards (PCBs) constituting its major ingredient. Results from the extraction of Cu and Ni from PCBs using biogenic $Fe_2(SO_4)_3$ obtained from the original isolate *Acidithiobacillus ferrooxidans* 61 (KM819692) are presented. *At. ferrooxidans* 61 was grown at a temperature of 30 °C in a modified 9 K medium supplemented with ferrous iron. Two-stage bioleaching was carried out at 600 rpm and 40 °C. Experiments were performed at 10% of pulp density (PD) with 48-h duration (each stage of 24 h), under pH 1 and 20 g/L Fe^{3+}. Under these conditions, overall recovery of Cu and Ni of 95% and 87% respectively was achieved. The obtained results indicate that non-ferrous metals in PCBs may be efficiently leached within two-stage bioleaching coupling bio-oxidation to subsequent redoxolysis. Scanning electron microscope (SEM) images acquisition and elemental mapping were performed to assess the liberation degree of essential phases after size-reduction steps and their implication on bioleaching efficiency.

1. Introduction

The generated volume of electronic waste (*E*-waste) is linked to the rapid technological innovation taking place nowadays and the corresponding growing demand inside the electronics sector. Shortening of electronic devices economic lifespan, lack of international agreement on *E*-waste management, and insufficient user awareness have all contributed to an unprecedented increase in accumulated *E*-waste (Naseri et al., 2022a; Vermeşan et al., 2019; Beiki et al., 2023).

According to recent reports, global *E*-waste production in 2021 was 52.2 million metric tons (Mt) and is expected to exceed 120 Mt. by 2050 (Kumar et al., 2021; Naseri et al., 2022b). Spent printed circuit boards (PCBs) form one of the most important streams in the global *E*-waste flux in terms of intrinsic value, although they account for merely 3%–6% (by weight) of total E-waste (Kumar et al., 2017). In 2014, approximately 2 Mt. of this waste was generated. Furthermore, the amount of spent PCBs grows in lockstep with the global increase in E-waste.

End-of-life PCBs are a complex assemblage of metals (nonferrous and ferrous), polymers (epoxy resin or fiberglass-based, various silicate-based phases), and ceramics (Sahan et al., 2019). The improper disposal of PCBs can result in the release of potentially toxic elements into the atmosphere, water, and soil, causing food chain toxicity risks (Wang et al., 2017a, 2017b).

Recycling this waste bears a direct environmental benefit while providing significant economic incentives (Pokhrel et al., 2020). The latter is because spent PCBs could be sourced for valuable metals given their average grades: 8–38% Fe, 10–27% Cu, 2–19% Al, 1–3% Pb, 0.3–2% Ni, 200–3000 g/t Ag, 20–500 g/t Au, and platinum group metals (10–200 ppm Pd) (Pokhrel et al., 2020). PCBs are classified into three categories based on their gold tenor: low (<100 ppm), medium (100–400 ppm), and high (>400 ppm) (Hagelueken, 2006; Kaya, 2016).

It is an acknowledged fact that metal grades in spent PCBs are significantly higher than in mineral ores (Cui and Zhang, 2008), therefore metal recovery from spent PCBs deserves much more consideration.

Abbreviations: *E*-waste, electronic waste; PCBs, printed circuit boards; PD, pulp density; SEM, scanning electron microscope; EDS, energy dispersive spectroscopy; BSE, backscattered electrons; Mt, million metric tons; XRD, X-ray diffraction; FT-IR, Fourier transform infrared spectroscopy; Fe(III), ferric iron; Fe(II), ferrous iron; MPN, most probable number; PLS, pregnant leach solution; EDTA, ethylenediaminetetraacetic acid; ICP-OES, inductively coupled plasma optical emission spectroscopy.

* Corresponding author at: SPC "Armbiotechnology" of National Academy of Sciences of Armenia, Gyurjyan 14, Yerevan 0056, Armenia.
E-mail addresses: arevik.vardanyan@asnet.am, avardanyan@uliege.be (A. Vardanyan), nvard@sci.am (N. Vardanyan), S.Gaydardzhiev@uliege.be (S. Gaydardzhiev).

https://doi.org/10.1016/j.hydromet.2023.106145
Received 30 March 2023; Received in revised form 24 July 2023; Accepted 7 August 2023
Available online 9 August 2023

Pyrometallurgical, hydrometallurgical, and biohydrometallurgical methods are used to recycle spent PCBs (Naseri and Mousavi, 2022; Xolo et al., 2021; I¸sıldar et al., 2016; Baniasadi et al., 2019; Krishnan et al., 2021; Zhou et al., 2009).

Brominated flame retardants, polybrominated biphenyls, tetrabromobisphenol-A, and polybrominated diphenyl ethers are among the hazardous and toxic pollutants found in *E*-waste. These are classified as persistent organic pollutants because they are highly toxic, stable, and bio-accumulative (Is¸ildar et al., 2018; Khanna et al., 2020; Robinson, 2009; Mir and Dhawan, 2022).

Reviews on PCB recycling have primarily focused on hydrometallurgical processes (Akcil et al., 2015; Cui and Anderson, 2016; Sethurajan et al., 2019; Tabelin et al., 2021; Tuncuk et al., 2012), pyrometallurgical processes (Tabelin et al., 2021; Wang et al., 2017b), pre-treatment approaches (Kang et al., 2021; Kaya, 2016; Moyo et al., 2020; Qiu et al., 2020), and gold recovery (Rao et al., 2020; Syed, 2012). However, very few focused on comprehensive metal recycling processes (Hao et al., 2020), and to our best knowledge none of them deals with the recycling of electronic components (an integral component) of PCBs or the generation of value-added end-products.

The complicated structure (due to regular model upgrades) and design of PCBs, as a result of the consolidated amalgamation of different elements (valuables, hazardous, inert) make separation and, thus, material recovery difficult. Furthermore, such a heterogeneous, non-uniform compositional design presents a significant sampling challenge, and sampling results are frequently not a true reflection of the elemental composition. The tendency of constituents to exhibit different mechanical responses creates uncertainty because the estimation of grades (composition) is highly dependent on the particle size and sample mass used in analytical routines (Touze et al., 2020).

There is no proper characterization technique to quantitatively evaluate the spatial difference and heterogeneous distribution or the liberation/association of different components without performing rigorous or energy-intensive milling (Otsuki et al., 2020). X-ray diffraction (XRD), inductively coupled plasma (ICP) spectrometry, and scanning electron microscopy/energy dispersive spectroscopy (SEM/EDS) are used to identify inclusive phases, morphology, structure, and compositional analysis of feeds, pre-treated products, or leach residues. Fourier transform infrared spectroscopy (FT-IR) of solutions is typically used to analyze the chemistry of regenerated solvents using the standard KBr method (Verma et al., 2017).

Size reduction is required for the effective liberation of metal-bearing carriers from associated non-metallic constituents in PCBs; the process is accomplished through a variety of mechanical equipment. As a rule, following milling down to 150 μm, complete liberation of metallic and non-metallic values in PCBs was observed (Vidyadhar and Das, 2013). After one or two steps of grinding, metals report mostly in size fractions of below 1000 μm, according to other studies (Arshadi et al., 2018; Kaya, 2016). A cryo-milling process (−119 °C) was also investigated to obtain nano-sized particles (metals, metal oxides, and nonmetals) (Tiwary et al., 2017). Mechanical size reduction processes, however, are notoriously known to consume energy and are associated with the loss of precious metals in the dust fractions (Barnwal et al., 2020; Zhou and Qiu, 2010).

Bioleaching technology has the potential to become an environmentally friendly method for metals recycling from *E*-wastes. It has been extensively tested, notably in the extraction of metals from low-grade ores (Dorado et al., 2012) and, more recently, from E-waste (Valix et al., 2001; Brandl et al., 2008; Mishra et al., 2008; Ivanus, 2010; Hong and Valix, 2014). Because of their ability to facilitate metal dissolution via a series of bio-oxidation reactions, various chemolithotrophic microorganisms are used in bioleaching applications (Hong and Valix, 2014; Modin et al., 2017; Brandl et al., 2001; Yang et al., 2017; Zhu et al., 2011; Xia et al., 2017). Inside the bioleaching system, iron serves as an electron acceptor. The oxidized form of ferric iron (Fe(III)), produced by the microbial oxidation of ferrous iron (Fe(II)) substrate, functions as an oxidant capable of oxidizing metal sulfides before being chemically reduced to ferrous iron via redoxolysis (Mahmoud et al., 2017). Acid leaching is supported by acidophilic autotrophs such as *Acidithiobacillus thiooxidans* (Murugesan et al., 2020; Vardanyan et al., 2022b), which produce sulphuric acid in the presence of thiosulphate/sulfur/sulfide, whereas bio-oxidation is performed by acidophilic iron-oxidizing autotrophs such as *Acidithiobacillus ferrooxidans* (Sodha et al., 2019; Ilyas et al., 2007; Vardanyan et al., 2022a, 2022b), *Leptospirillum ferrooxidans* (Sodha et al., 2019) and *Leptospirillum ferriphilum* (Anaya-Garzon et al., 2021).

Several studies (Bas et al., 2013; Guezennec et al., 2018; Ilyas et al., 2010; Sodha et al., 2020) have been published on the feasibility of PCBs bioleaching in batch mode using shake flasks and bioreactors. However, due to their notorious heterogeneity, PCBs bioleaching should ideally be investigated using large-volume stirred tank reactors (>1 L), which can handle a sufficient amount of material and offer an upscaling platform. Such conditions ensure efficient reactant transport and closely resemble industrial situations (Hubau et al., 2020). Staggered addition of PCBs with continuous biological production of an acidic lixiviant containing Fe(III) improves bioleaching efficiency, most likely due to reduced PCB toxicity on microbial growth (Brandl et al., 2001; Hubau et al., 2020; Liang et al., 2013).

Metal toxicity effects on microbial growth can be addressed using an indirect leaching approach that decouples lixiviant production and *E*-waste leaching. This two-stage concept has been successfully demonstrated under a laboratory scale for the leaching of metals from lithium-ion batteries (Boxall et al., 2018) and PCBs (Hubau et al., 2020; Yken et al., 2020; Vardanyan et al., 2022a).

The degree of liberation indicating what amount of the targeted component is liberated from the non-valuable PCBs matrix is an important factor in determining the success of the subsequent valuable materials recovery stage (Das et al., 2009). This key parameter was first embraced by the mineral processing industry, with a goal to achieve selective liberation of the minerals of interest at the coarsest particle size possible, thus saving energy on the grinding process and reducing the generated amount of undesirable fine fractions (Wills and Finch, 2016; Ueda et al., 2017). In contrast to primary ore beneficiation, a specific size range guarantying the optimum liberation of valuable metals from non-metallic fractions in a discarded PCB assemblage is still unknown. Published researches investigate the effect of particle size and shape on liberation characteristics (Zhang and Forssberg, 1999; Koyanaka et al., 2006), and high liberation degrees were reported with particle sizes below 100 μm or between 100 μm and 3 mm. Such disparities could be most likely attributed to the differences in PCBs origin and hence compositions and likewise to the size reduction equipment used in comminution processes (Chao et al., 2011).

In view of the aforementioned, the current study aims to investigate the recovery of copper and nickel from PCBs using culture-bearing solutions derived from an acidophilic iron-oxidizing bacterium, *Acidithiobacillus ferrooxidans* 61. To counteract the potential toxicity of PCBs on microbial growth and activity, an indirect bioleaching approach practiced in double-stage mode was chosen. Metal leaching efficiency was expected to increase by decoupling biolixiviant generation and bioleaching steps. To follow material transformation patterns specific fractions from the process were subjected to SEM-EDS inspection.

2. Materials and methods

2.1. Printed circuit board preparation

End-of-life PCBs delivered by the EXITCOM company based in Turkey were manually depopulated and fragmented down to a particle size below 22 mm by a hammer mill (Laarmann CHM4000) run at 1750 rpm. The analysis of the input PCBs revealed the following concentrations of principal non-ferrous metals: Cu (24.6%), Zn (0.08%), Ni (0.1%), and Al (2.6%). The surface passivation layer (green lacquer

mask) was removed before the bioleaching by boiling the depopulated PCBs in a 10% NaOH solution for 15 min at S/L ratio of 20. The samples were washed with deionized water until neutral pH, dried at room temperature, and preserved for leaching.

2.2. Biogeneration of lixiviant

The biolixiviant used for leaching was obtained using an iron-oxidizing culture *Acidithiobacillus ferrooxidans* 61 (KM819692) isolated from Tandzut ore (Armenia) acid drainage water (Vardanyan et al., 2015). *At. ferrooxidans* 61 was grown in modified 9 K medium (0.5 g/L $(NH_4)_2SO_4$, 0.5 g/L $MgSO_4 \times 7H_2O$, 0.5 g/L K_2HPO_4, 0.05 g/L KCl, 0.01 g/L $Ca(NO_3)_2$) containing 25 gL^{-1} ferrous iron (supplemented as $FeSO_4 \times 7H_2O$). The growth of bacteria as described previously (Vardanyan et al., 2022a) was carried out inside a bio-fermenter (Bionet Baby 0) coupled to a control unit, to follow gas supply, stirring rate, pH, Eh, and temperature. The fermenter filled in with 2 L medium was inoculated at 10% (*v*/v) with bacterial culture and pH adjusted to 1.8–1.9 using 10 N H_2SO_4. The fermenter was operated at a temperature of 30 °C, stirring speed of 80 rpm, and 1 L/min air-flow. After 5–7 days of cultivation, a reddish coloration of the culture medium was observed due to oxidation of Fe^{2+} to Fe^{3+}. The redox potential of the lixiviant was around 700 mV (Ag/AgCl ref.) with cell enumeration staying in the range of 2.5×10^8 cells/mL. The quantitative determination of bacterial cells (enumeration) was carried out by a serial end-point dilution technique known as the "most probable number" (MPN) method (Erkmen, 2022).

2.3. Bioleaching experiments

Two-stage bioleaching of ground ≤2 cm size fraction of the PCBs was performed inside a 2-L jacketed reactor coupled to a circulating bath maintaining a constant operating temperature of 40 °C required to sustain eventual bacterial growth. The reactor was connected to a condenser to prevent excessive evaporation and a tunable compressor to supply air (Vardanyan et al., 2022a). Leaching experiments were performed under starting pH of 1 (10 N H_2SO_4 was used for pH adjustment) and 20 g/L of Fe^{3+} as an oxidizing agent. The duration of the bioleaching experiment was 48 h, with each stage being fixed to 24 h. To realize this, after elapsing the first 24 h of leaching, the pregnant leach solution (PLS) was decantated and fresh lixiviant was added to the reactor. Solution sampling was performed at start of the experiment, and further at 1 h, 2 h, 3 h, 4 h, 5 h, 6 h, 7 h, and 24 h of each stage. After bioleaching, the residue was recovered as two different granulometric fractions: "coarse" (1–2 mm) and "fine" (below 1 mm). The "coarse" fraction was obtained after sieving, while the "fine" fraction was the one remaining on the paper filter after the vacuum filtration of the PLS. Following separation, "coarse" and "fine" fractions were dried and used for microscopic inspection.

2.4. Scanning electron microscopy (SEM) and energy dispersive X-ray spectroscopy (EDS)

PCBs were observed with respect to morphology, chemistry and phases liberation by a SEM-based automated mineralogy system - Zeiss sigma 300 FEG "Mineralogic" coupled to two Brucker EDS x Flash 6|30 X-ray energy dispersion spectrometers (silicon drift detector). To this end, raw PCBs and leached samples were cast into 30 mm diameter mounts following an established procedure (Bouzahzah et al., 2015). The section polishing was accomplished by polishing disks and diamond suspensions of different finesses. The SEM-EDS analyses were carried out using a probe current of 2.3 nA with an accelerating voltage of 20 kV at a working distance of 8.5 mm. A mapping mode was performed using a 3 to 5 μm step size and a dwell time of 55 ms. Analytical conditions such as contrast and brightness were set up manually to provide the best possible contrast between the observed phases (plastics, composites, metals). System magnification was set to 6000 X and voltage tension to 20 kV.

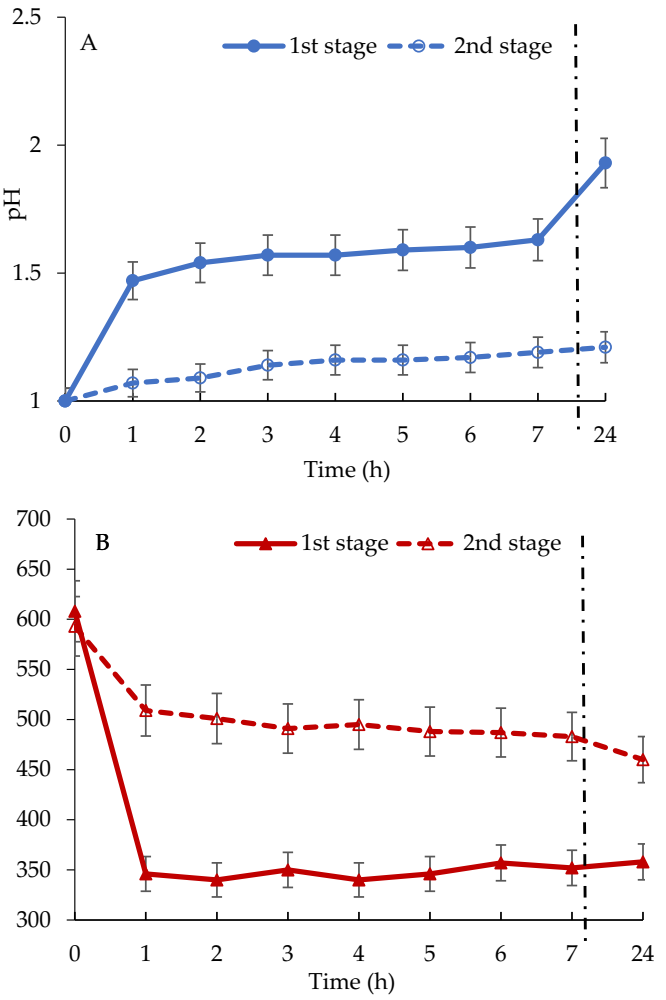

Fig. 1. Variation of pH (A) and ORP (B) during bioleaching of PCBs (PD 10%, initial pH - 1, Fe^{3+} – 20 g/L, 40 °C, air - 1 L/min, 600 rpm, overall duration - 48 h (each stage 24 h)).

2.5. Analytical determination

Metals in the pregnant leach solution (PLS) were analyzed by inductively coupled plasma optical emission spectroscopy (ICP-OES). The solid residue after leaching was dried, oven treated at 900 °C for 240 min, ground in an agate mortar or a ring mill, and digested in aqua regia before being analyzed, similar to the liquid samples. Ferrous and ferric iron concentration was determined by an ethylenediaminetetraacetic acid (EDTA) based complexometric titration (Lucchesi and Hirn, 1960). Mineralogical inspection of the leached PCBs was realized on a Bruker (Billerica, MA, USA) D8 ECO diffractometer using CuK α radiation (λ = 1.5418 Å). A representative amount of the material was pulverized in an agate mortar and then deposited on a zero-background silicon sample holder. The X-ray powder diffraction patterns were first interpreted using the EVA 3.2 software. This software allowed us to identify the phases and compare them to the International Centre for Diffraction Data (ICDD) database, version PDF-2. Then, the powder patterns were analyzed using the TOPAS 4.2 software which allowed quantification of the mineral phases. The quantification procedure is based on the Rietveld method.

Two replicates of tests were conducted. The standard deviation was calculated using STDEV·S function available in MS Excel and error bars were added.

Table 1
Bacteria enumeration during the bioleaching (PD 10%, initial pH - 1, Fe^{3+} – 20 g/L, 40 °C, air – 1 L/min, 600 rpm, duration - 24 h).

Duration (h)	Number of cells (cells/mL)
0	2.5×10^8
1	0.6×10^7
3	2.5×10^2
5	N/D*
24	N/D

* N/D – not detected.

3. Results and discussion

3.1. Two-stage bioleaching of printed circuit boards (PCBs)

In our previous experiments, we studied the effect of different oxidizing agent (Fe^{3+}) concentrations, varying pH, and pulp density (PD) on metal extraction efficiency (Vardanyan et al., 2022a). In this study, apart characterising feed and residue material after bioleaching, PCBs were subjected to a two-stage subsequent bioleaching via biologically obtained Fe^{3+} by *At. ferrooxidans* 61. 10% of PD was chosen as to approach industrially relevant conditions. The entire two-stage bioleaching (24 h + 24 h) at 10% PD, pH 1, and 20 gL^{-1} ferric iron, has secured metal recoveries of 95% for Cu and 87% for Ni and almost complete recovery for Zn (data not presented). The recovery of Al was about 3% (data not shown) which corresponds to our previous findings (Vardanyan et al., 2022a). This low recovery level is most likely due to the intrinsic refractoriness of the aluminum met in PCBs (e.g., as an alloy), and the presence of surface coatings or encapsulation within the PCB matrix.

Fig. 1A shows that the initial pH increases during the bioleaching process. This phenomenon could be explained by the proton consumption reactions (1–9), the main ones presented below:

$$Ni^0 + 2Fe^{3+} \rightarrow Ni^{2+} + 2Fe^{2+} \quad (1)$$

$$2Fe^{2+} + 0.5O_2 + 2H^+ \rightarrow 2Fe^{3+} + H_2O \quad (2)$$

$$\text{Sum of the two reactions} : Ni^0 + 0.5O_2 + 2H^+ \rightarrow Ni^{2+} + H_2O \quad (3)$$

$$Al^0 + 3Fe^{3+} \rightarrow Al^{3+} + 3Fe^{2+} \quad (4)$$

$$2Fe^{2+} + 0.5O_2 + 2H + \rightarrow 2Fe^{3+} + H_2O \quad (5)$$

$$\text{Sum of the two reactions} : Al^0 + 0.5O_2 + 2H^+ \rightarrow Al^{3+} + H_2O \quad (6)$$

$$Cu^0 + 2Fe^{3+} \rightarrow Cu^{2+} + 2Fe^{3+} \quad (7)$$

$$2Fe^{2+} + 0.5O_2 + 2H^+ \rightarrow 2Fe^{3+} + H_2O \quad (8)$$

$$\text{Sum of the two reactions} : 2Cu^0 + O_2 + 4H^+ \rightarrow 2Cu^{2+} + 2H_2O \quad (9)$$

It is reasonable to assume, that the zero valence metals may have been directly chemically or biologically leached, according to reactions (10) and (11), with the resulting hydroxide ions being responsible for the increase in pH during the leaching process (Fu et al., 2016; Pourhossein and Mousavi, 2018; Tapia et al., 2022).

$$4M^0 + 12H^+ + 3O_2 \rightarrow 4\,M^{3+} + 6H_2O \quad (10)$$

$$2M^0 + 2H_2O + O_2 \rightarrow 2\,M^{2+} + 4OH^- \quad (11)$$

As shown in Fig. 1A, the initial pH increases from 1 to 1.9 in the first, but drops back to 1.2 in the second stage, respectively. As pH was low, only limited amount of jarosite was detected during EDS mapping in the "coarse" fraction. It is assumed that the maximum recovery of metals takes place mainly during the first stage, which was likewise reported in our previous work (Vardanyan et al., 2022a). This explains the non-substantial variation in pH observed during the second stage of leaching.

The oxidation-reduction potential (ORP) is also an important parameter that reflects chemical reactions taking place during a leaching process. As shown in Fig. 1B, the ORP of the bacterial solution dropped sharply from 608 mV to 346 mV (Ag/AgCl), for 1 h of leaching due to the reduction of Fe^{3+} ions to Fe^{2+} (redoxolysis). During the second stage, ORP declined at a slower pace from 593 to 460 mV (Ag/AgCl), which proves the assumption that leaching takes place mainly in the first stage with the elevated ORP values indicating the prevalence of Fe^{3+} over Fe^{2+} in the lixiviant.

As shown in Table 1, after 3 h of leaching there was a distinct drop in bacterial population in the PLS - from 10^8 to 10^2 cells/mL. After 3 h of leaching no growth of bacteria was observed due to the inhibitory effect of PCBs on bacterial activity given their heterogenous composition carrying a variety of hazardous compounds and possibly due to the initial low pH.

3.2. Printed circuit boards (PCB) characterization by scanning electron microscopy (SEM) and energy dispersive X-ray spectroscopy (EDS)

It was important to assess and trace visually the evolution of PCB fragments and their morphology before and after leaching. The optical microscope images before and after bioleaching are shown in Fig. 2. As shown by the micrographs A and B, the bright and colored points depict metallic particles, which are almost leached as demonstrated by the "fine" fraction (image C) observation.

Due to the known disparities in phase composition, plastics (dark) and metallic (bright) spots may be distinguished in the backscattered

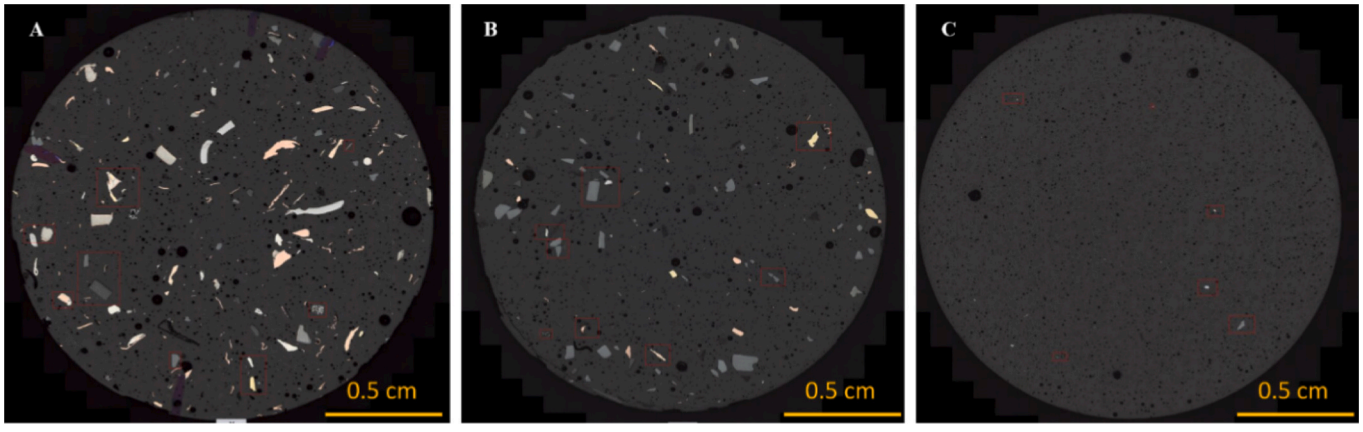

Fig. 2. Optical microscopic views of PCBs: before bioleaching (A), "coarse" fraction residue after bioleaching (B), and "fine" residue fraction after leaching (C).

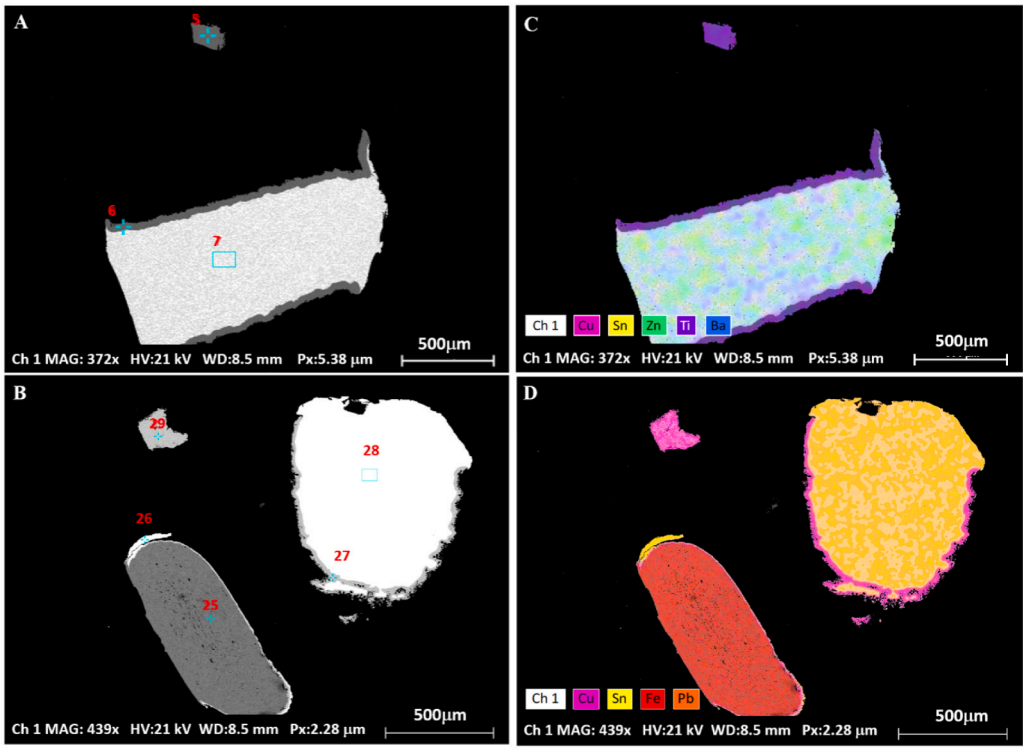

Fig. 3. Characteristic micrographs (BSE-SEM) (A, B) of solid phases belonging to feed PCBs; 5, 6 - Cu; 7- Cu–Sn-Pb alloy; 25 - Fe; 26 - Sn; 27, 29 - Cu; 28 - Sn—Pb alloy; EDS-SEM (C, D) elemental mapping.

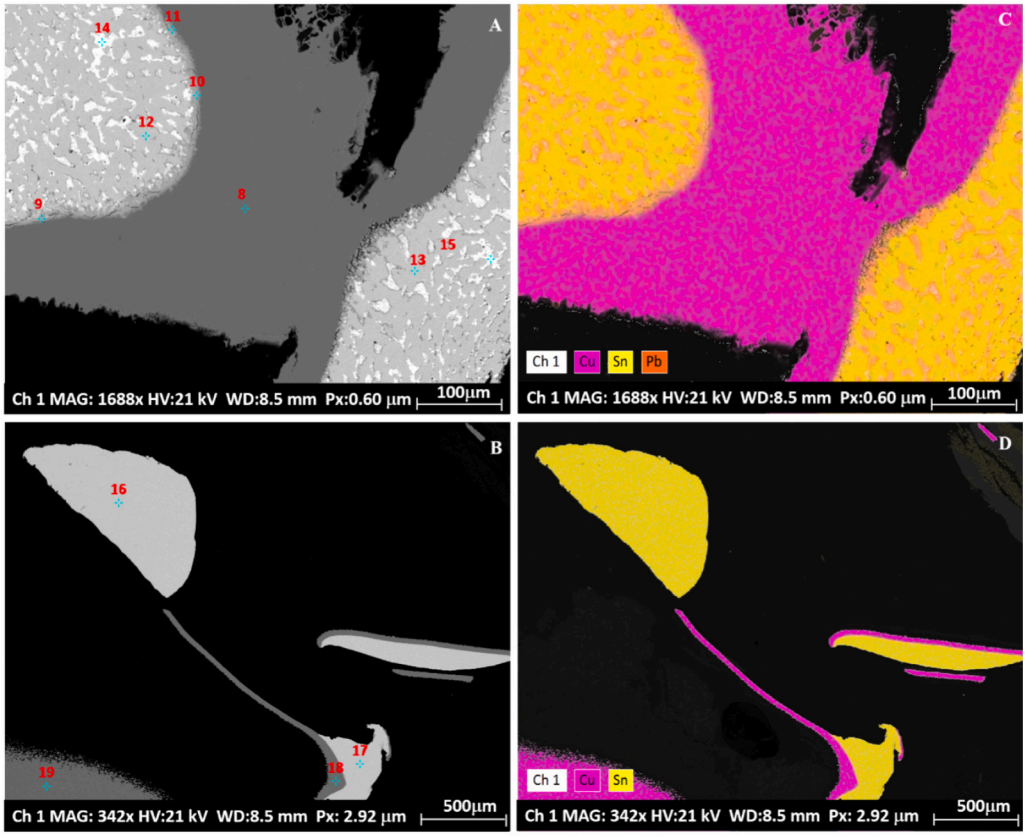

Fig. 4. Characteristic micrographs (BSE-SEM) of solid phases belonging to feed PCBs (A, B); 8, 18, 19 - Cu; 9–13, 16, 17 - Cu—Sn alloy; 14, 15 - Cu—Pb alloy. EDS-SEM (C, D) images showing elemental mapping.

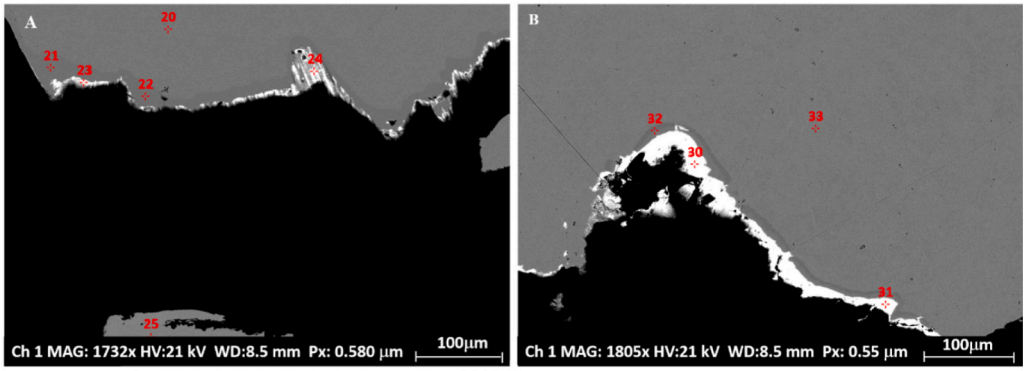

Fig. 5. Characteristic micrographs (BSE-SEM) of metals and alloys originating from feed PCBs (A, B), 20, 33 - Cu; 21, 22 - Ni; 23, 24, 32 - Ni-Cu-Au; 25 - Cu—Zn alloy; 30, 31 - Sn; 18, 19 - Cu; 9–13, 16, 17 - Cu—Sn alloy.

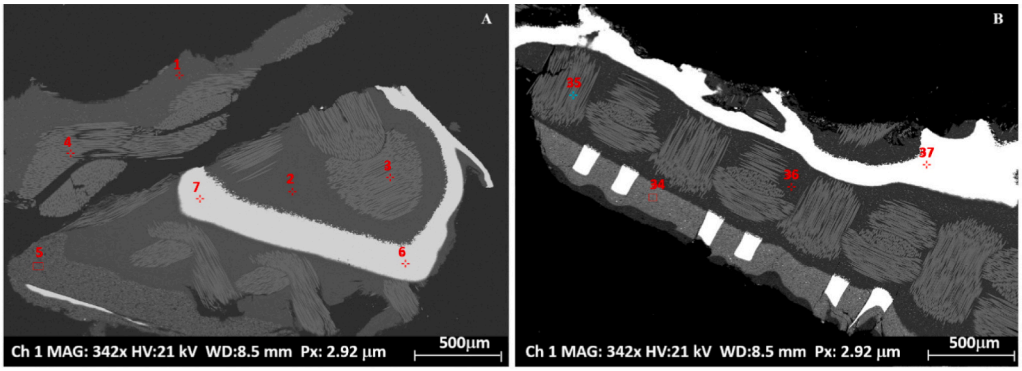

Fig. 6. Characteristic micrographs (BSE-SEM) of metals originating from feed PCBs; 1, 2 - Br; 3–5, 34–36 - Silicon with metals alloy; 6, 7, 18, 19, 20, 33, 37 - Cu; 21, 22 - Ni; 23, 24, 32 - Ni-Cu-Au; 25 - Cu—Zn alloy; 30, 31 - Sn; 9–13, 16, 17 - Cu—Sn alloy.

Table 2
EDS mapping of leached PCB (feed pictured in Fig. 5).

Spectrum	Metal content (%)				
	Ni	Cu	Zn	Au	Sn
20		100			
21	100				
22	100				
23	25.9	3.1		71.2	
24	43.5	4.2		52.4	
25		64.8	35.3		
30					100
31					100
32	100				
33		100			

Table 3
EDS mapping of leached PCB ("fine" fraction pictured in Fig. 8*).

Spectrum	Metal content (%)							
	Al	P	S	K	Ti	Fe	Sn	Pb
18					25.7			
19		6.7	0.9			12.9	48.9	
20	0.7					1.1	4.3	82.3
21		3.6	2.0			18.2	50.6	
22			13.9	6.4		35.4		
28	55.4							
29	1.1					0.6	2.5	95.8
30		3.1	2.4			18.7	45.3	
31		3.2	1.8			19.2	44.2	*

* -As Sr, Bi, K, Ti, and Silicon are not shown in Table 3.

electrons (BSE) images, which present signals from a polished section in greyscale. Commonly energy dispersive spectroscopy (EDS) is used to obtain additional information in order to differentiate the composition of the detected metallic particles. It is worth noting that PCBs have a multi-elemental base composition (Korf et al., 2019), so a large number of elements are expected to be found. The primary metals that comprise PCBs, according to an EDS mapping, are Cu, Zn, Sn, Ti, Ba, Pb, Fe and Au. It should be noted that these metals are usually met as alloys between each other.

Characteristic micrographs and microanalyses of the feed PCBs are shown in Figs. 3-6. These micrographs suggest a strong material heterogeneity, which corroborates the known multi-material nature of PCBs (Gonçalves and Otsuki, 2019). Different alloy phases were identified, namely Cu—Sn, Cu—Zn, Cu—Ni, as well as such with Fe and silicon. As illustrated in Fig. 3, non-liberated Cu (point 6 in Fig. 3A and point 27 in Fig. 3B) surrounds Sn and Pb bearing alloys (Supplementary Table 1) with round or irregular-shaped globules. The EDS mapping revealed that the copper fragments were also englobed by traces of jarosite and Zn (Supplementary Fig. 1, Table 1), the former probably originating from the alkaline composite matrix, the latter being part of the PCBs mainframe.

In Fig. 4 tin (Sn) is pictured, belonging more likely to a soldering material met in the fragmented PCBs as joined with copper assemblage fragment (points 9–13 mapped in Fig. 4A, Supplementary Table 2) or as a single fragment (point 16 and 17 mapped in Fig. 4B, Supplementary Table 2). Carelse et al., 2020 identified based on EDS analysis identified two Cu—Sn phases taking into account the Sn content of the feed material.

Fig. 5 and Table 2 reveal a non-liberated native Cu (point 20 mapped in Fig. 5A, and point 33 mapped in Fig. 5B) attached to Ni-Cu-Au alloys

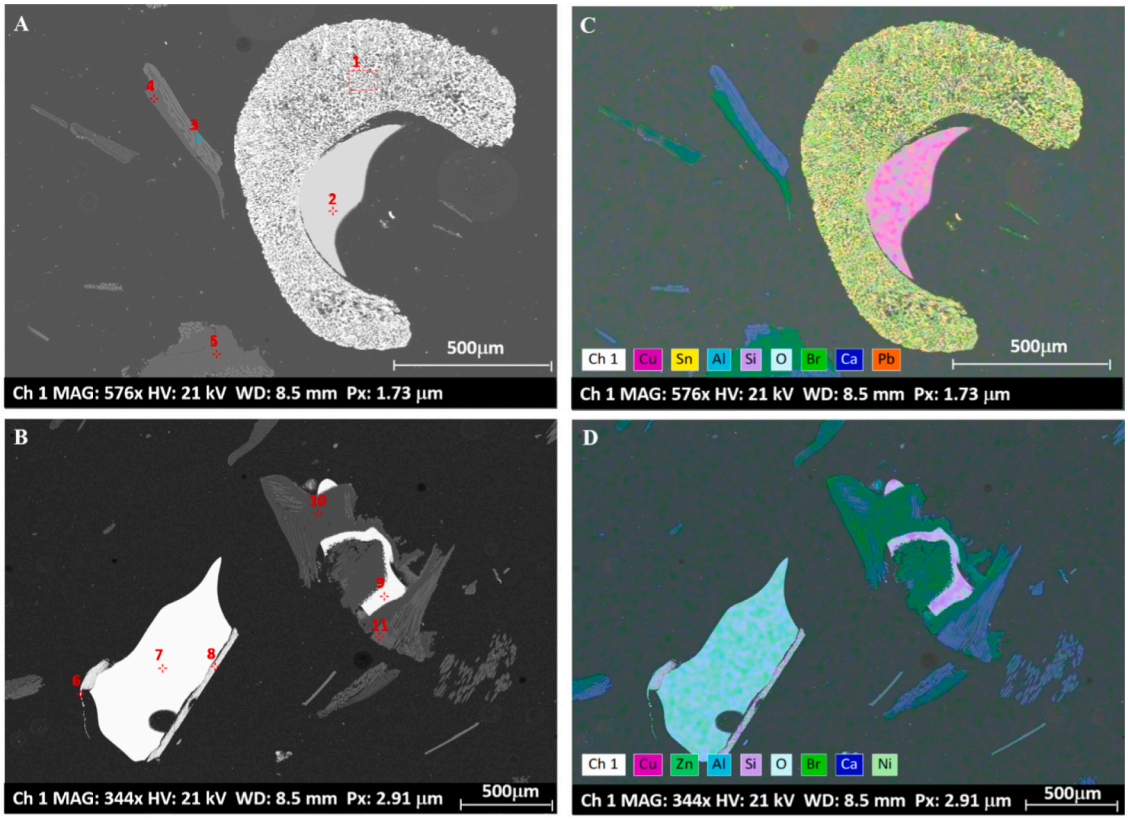

Fig. 7. Characteristic micrographs (BSE-SEM) of compounds found in leached PCBs ("coarse" fraction) (A, B), 1, 2 - Al-Cu-Sn-Pb alloy; 4, 5 - Br-Pb; 7, 8: Cu—Zn alloy; 9 - Cu; 10 - Cu—Br alloy; 3, 11 - Silicon with metals; 27 - Al-Cu-Sn alloy; 28, 29 - jarosite. EDS-SEM images (C, D) showing elemental mapping.

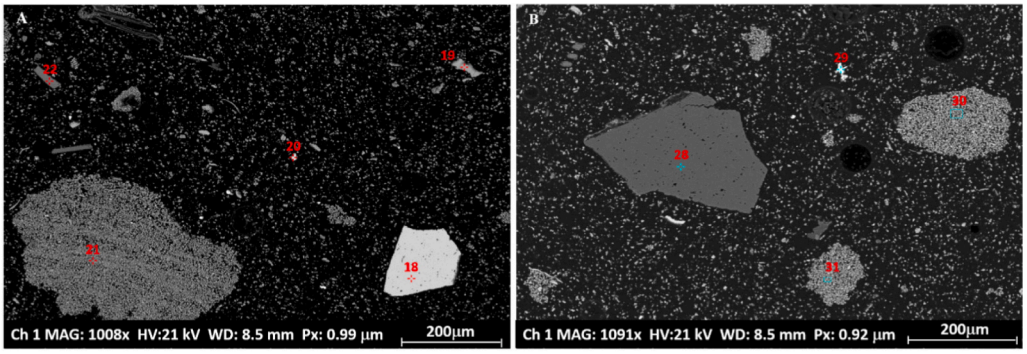

Fig. 8. Characteristic micrographs (BSE-SEM) analysis of metals and jarosite remnants in leached PCBs ("fine" fraction), 18 - Ti; 19, 21, 30, 31 - Sn, jarosite; 20, 29 - Sn—Pb alloy; 22 - jarosite; 28 - Al.

and also metallic Ni and Sn, respectively. Worth to note that spots having high silica content complexed to metallic particles are often detectable (Fig. 6, Supplementary Table 3). It could be assumed that the fiberglass-silica laminates encapsulate the metals, which following the attrition effects caused by the agitative leaching get eventually liberated. This ultimately leads to a relatively high metal liberation degree in the fine granulometric fractions, compared to the one observed in non-leached PCBs (feed material).

The micrographs and surface mapping of a sample leached by the lixiviant obtained from *At. ferrooxidans* 61 at 40 °C and 600 rpm for 48 h are pictured in Figs. 7 and 8. The Br detected in the leached material – Fig. 7A, originates by no doubt from a brominated flame-retardant coverage commonly used in PCBs to avoid flammability (Zhou et al., 2013). After leaching completion, the leached residue was recovered as two different granulometric fractions: "coarse" (1–2 mm) (Fig. 7) and "fine" (below 1 mm) (Fig. 8). It is supposed that the generation of "fine" fraction is result of bacterial activity. Hyra et al., 2022 also reported on the existence of a "fine" fraction (200 nm) in bioleaching residues, while in the case of chemical leaching, agglomerates being significantly larger (500 nm) were detected. The obtained results indicated bacterial activity in the solubilization process of metals with visible degradation of PCBs particles.

Fig. 7A and Supplementary Table 4 illustrate a Cu fragment interlocked with a Sn—Pb alloy. A small amount of Al and Br, as well as silica laminate were also detected. In Fig. 7B, Cu—Zn alloy being interlocked with Br and silica laminate (points 9, 10, 11) was detected, and another piece of Cu fragment was found to be surrounded by Ni and Cu—Zn alloy (points 6, 7, 8). Traces of jarosite and silica laminate were often found in the leached fraction, both of which were deposited on the PCB composite matrix (Supplementary Fig. 2, Supplementary Tables 4, 5). Zero-

valent Cu, Ni, and Zn appear to have been released to some extent by the liberation-inducing fragmentation, but some of them were apparently trapped inside the PCB stacking. The results indicate that possible passivation phenomena happen during the leaching or that the hydrodynamic conditions inside the reactor were not ideal, potentially maintaining dead zones and allowing part of the material to escape from contact with the lixiviant. The remaining "fine" grained material after leaching was heterogeneous, made up of a mixture of all refractory-to-leaching components found in the PCBs. The aforementioned findings might be the reason for the non-complete Cu and Ni extraction in the "coarse" fraction. The EDS data for the spots flagged in Fig. 8 are displayed in Table 3.

As shown in Table 3, PCBs "fine" fraction has lower metallic deportment, likely due to the fact that metallic substances are generally ductile in nature and do not shatter easily into dust fines during comminution in contrast to their non-metallic counterparts. The EDS analysis has not detected non-ferrous metals (Cu, Ni) in the "fine" fraction of the leached residue, supporting the almost complete recovery of these metals by the biolixiviant under the tested conditions. There is a clear trend of higher liberation of metals from the PCBs matrix towards the "fine" fraction. This trend agrees with previous studies (Gonçalves and Otsuki, 2019; Otsuki et al., 2019a). Otsuki et al., 2019b reported that "coarse" fractions (0.125–2 mm) are more complex than "fine" fractions (<0.5 mm) where agglomerates do not exist. Park et al., 2018 reported similar observations suggesting liberation of metals increase with particle size decrease.

4. Conclusions

Conditions that have previously (Vardanyan et al., 2022a) been found to be optimal (pH 1, 10% PD, and 20 g/L Fe^{3+}) were used for a two-stage bioleaching of PCBs which allowed reaching up to 95% extraction of copper, 87% of Ni and an almost complete extraction of Zn in 48 h. The results obtained indicate that metals in PCBs may be efficiently leached by a two-stage process involving bio-oxidation coupled to subsequent redoxolysis.

The micrographs of the input and output products from the leaching witnessed a diverse morphology and level of metal-bearing compounds liberation while the microanalysis confirmed the presence of several metals: Cu, Zn, Ni, Sn, Pb, Zn, Au and Al. Microscopic examination showed that the metals inside the "coarse" fraction of the leached residue were not fully liberated from the matrix, which provokes incomplete leaching. The intrinsic form under which metals are present in the PCBs (alloys, oxides, etc.) plays an essential role in their leachability. The EDS analysis has not detected Cu and Zn in the "fine fraction" (<1 mm) of the leached residue, supporting that the granulometric preparation of the feed material plays a key role for a complete extraction of metals from PCBs. A compromise should be however found between the efforts to grind the feed to a very fine size (< 1 mm) range and the potential economic gain due to an additional metals recovery.

Once Cu, Ni and Zn have been removed the concentration of As, Sr, Bi, and Ti becomes relatively high in the leached material which might require specific handling or prevent valorization. The morphological inspection of the leached material indicated jarosite-covered surfaces due to the precipitation of alkali metals during the bioleaching regardless of the low pH value.

Upon size reduction by comminution, only partial release of the metals from the PCBs silicate matrix was observed as witnessed from the SEM-EDS images. Nevertheless, during the leaching, material weakening might take place leading to an enhanced metal dissolution at the end. Thus, the degree of bringing metals into solution depends not only on the leaching conditions, but also on the level of metal liberation. Therefore, the size-reduction step has to be judiciously chosen as to liberate metals-bearing phases from the PCB matrix to a reasonable extent and expose them to the leaching agent.

Funding

The work was supported by ERAMIN-2 within the BaCLEM project (Walloon region grant N° 2010023) and the Science Committee of the Republic of Armenia, in the frame of the research project N° 21T-1F124.

CRediT authorship contribution statement

Arevik Vardanyan: Conceptualization, Methodology, Software, Formal analysis, Investigation, Writing – original draft, Visualization. **Narine Vardanyan:** Conceptualization, Validation, Writing – review & editing. **Stoyan Gaydardzhiev:** Conceptualization, Validation, Resources, Data curation, Supervision, Writing – review & editing, Project administration, Funding acquisition.

Declaration of Competing Interest

The authors declare no conflict of interest.

Acknowledgments

A.K. Vardanyan is grateful to the Wallonia-Brussels International (WBI) Postdoctoral Excellence Grant. The authors are thankful to H. Bouzahzah for the SEM-EDS analysis and interpretations.

Appendix A. Supplementary data

Supplementary data to this article can be found online at https://doi.org/10.1016/j.hydromet.2023.106145.

References

Akcil, A., Erust, C., Gahan, C. Sekha, Ozgun, M., Sahin, M., Tuncuk, A., 2015. Precious metal recovery from waste printed circuit boards using cyanide and non-cyanide lixiviants–a review. Waste Manag. 45, 258–271. https://doi.org/10.1016/j.wasman.2015.01.017.

Anaya-Garzon, J., Hubau, A., Joulian, C., Guezennec, A.G., 2021. Bioleaching of E-waste: influence of printed circuit boards on the activity of acidophilic Iron-oxidizing Bacteria. Front. Microbiol. 12, 669738 https://doi.org/10.3389/fmicb.2021.669738.

Arshadi, M., Yaghmaei, S., Mousavi, S.M., 2018. Content evaluation of different waste PCBs to enhance basic metals recycling. Resour. Conserv. Recycl. 139, 298–306. https://doi.org/10.1016/j.resconrec.2018.08.013.

Baniasadi, M., Vakilchap, F., Bahaloo-Horeh, N., Mousavi, S.M., Farnaud, S., 2019. Advances in bioleaching as a sustainable method for metal recovery from e-waste: a review. J. Ind. Eng. Chem. 76, 75–90. https://doi.org/10.1016/j.jiec.2019.03.047.

Barnwal, A., Mir, S., Dhawan, N., 2020. Processing of discarded printed circuit board fines via flotation. J. Sustain. Metall. https://doi.org/10.1007/s40831-020-00304-4.

Bas, A.D., Deveci, H., Yazici, E.Y., 2013. Bioleaching of copper from low grade scrap TV circuit boards using mesophilic bacteria. Hydrometallurgy 138, 65–70. https://doi.org/10.1016/j.hydromet.2013.06.015.

Beiki, V., Naseri, T., Mousavi, S.M., 2023. Comprehensive characterization and environmental implications of spent telecommunication printed circuit boards: towards a cleaner and sustainable environment. J. Environ. Manag. 325, 116482 https://doi.org/10.1016/j.jenvman.2022.116482.

Bouzahzah, H., Benzaazoua, M., Mermillod-Blondin, R., Pirard, E., 2015. A novel procedure for polished section preparation for automated mineralogy avoiding internal particle settlement. In: Proceedings of the 12th International Congress for Applied Mineralogy (ICAM), Istanbul, Turkey, 10–12 August 2015.

Boxall, N.J., Cheng, K.Y., Bruckard, W., Kaksonen, A.H., 2018. Application of indirect non-contact bioleaching for extracting metals from waste lithium-ion batteries. J. Hazard. Mater. 360, 504–511. https://doi.org/10.1016/j.jhazmat.2018.08.024.

Brandl, H., Bosshard, R., Wegmann, M., 2001. Computer-munching microbes: metal leaching from electronic scrap by bacteria and fungi. Hydrometallurgy 59, 319–326. https://doi.org/10.1016/S0304-386X(00)00188-2.

Brandl, H., Lehmann, S., Faramarzi, M.A., Martinelli, D., 2008. Biomobilization of silver, gold, and platinum from solid waste materials by HCN-forming microorganisms. Hydrometallurgy 94, 14–17. https://doi.org/10.1016/j.hydromet.2008.05.016.

Carelse, C., Manuel, M., Chetty, D., Corfield, A., 2020. Au and ag distribution in alloys produced from the smelting of printed circuit boards – an assessment using SEM-EDS, EPMA, and LA-ICP-MS analysis. J. Southern Afr. Instit. Minin. Metall. 120, 203–210. https://doi.org/10.17159/2411-9717/698/2020.

Chao, G., Hui, W., Wei, L., Jiangang, F., Xin, Y., 2011. Liberation characteristic and physical separation of printed circuit board (PCB). Waste Manag. 31, 2161–2166. https://doi.org/10.1016/j.wasman.2011.05.011.

Cui, H., Anderson, C.G., 2016. Literature review of hydrometallurgical recycling of printed circuit boards (PCBs). J. Adv. Chem. Eng. 6 https://doi.org/10.4172/2090-4568.1000142.
Cui, J., Zhang, L., 2008. Metallurgical recovery of metals from electronic waste: a review. J. Hazard. Mater. 158, 228–256. https://doi.org/10.1016/j.jhazmat.2008.02.001.
Das, A., Vidyadhar, A., Mehrotra, S.P., 2009. A novel flowsheet for the recovery of metal values from waste printed circuit boards. Resour. Conserv. Recycl. 53, 464–469. https://doi.org/10.1016/j.resconrec.2009.03.008.
Dorado, A.D., Sole, M., Lao, C., Alfonso, P., Gamisans, X., 2012. Effect of pH and Fe (III) ions on chalcopyrite bioleaching by an adapted consortium from biogas sweetening. Miner. Eng. 39, 36–38. https://doi.org/10.1016/j.mineng.2012.06.009.
Erkmen, O., 2022. Practice 4 - Most probable number technique. In: Microbiological Analysis of Foods and Food Processing Environments. Elsevier, Amsterdam, The Netherlands, pp. 31–37.
Fu, K., Wang, B., Chen, H., Chen, M., Chen, S., 2016. Bioleaching of Al from coarse-grained waste printed circuit boards in a stirred tank reactor. Procedia Environ. Sci. 31, 897–902.
Gonçalves, P.P., Otsuki, A., 2019. Determination of liberation degree of mechanically processed waste printed circuit boards by using the digital microscope and SEM-EDS analysis. Electronics 8, 1202. https://doi.org/10.3390/electronics8101202.
Guezennec, A.G., Joulian, C., Delort, C., Bodenan, F., Hedrich, S., d'Hugues, P., 2018. CO2 mass gtransfer in bioleaching reactors: CO2 enrichment applied to a complex copper concetrate. Hydrometallurgy 180, 277–286. https://doi.org/10.1016/j.hydromet.2018.08.006.
Hagelueken, C., 2006. Recycling of electronic scrap at Umicore precious metals. Acta Metall. Slovaca 12, 111–120.
Hao, J., Wang, Y., Wu, Y., Guo, F., 2020. Metal recovery from waste printed circuit boards: a review for current status and perspectives. Resour. Conserv. Recycl. 157 https://doi.org/10.1016/j.resconrec.2020.104787.
Hong, Y., Valix, M., 2014. Bioleaching of electronic waste using acidophilic sulfur oxidizing bacteria. J. Clean. Prod. 65, 465–472. https://doi.org/10.1016/j.jclepro.2013.08.043.
Hubau, A., Minter, M., Changes, A., Joulian, C., Silvente, C., Guezennec, A.G., 2020. Recovery of metals in a double-stage continuous bioreactor for acid bioleaching of printed circuit boards (PCBs). Sep. Purif. Technol. 238, 116481 https://doi.org/10.1016/j.seppur.2019.116481.
Hyra, K., Nuckowski, P.M., Willner, J., Suponik, T., Franke, D., Pawlyta, M., Matus, K., Kwa'sny, W., 2022. Morphology, phase and chemical analysis of leachate after bioleaching metals from printed circuit boards. Materials 15, 4373. https://doi.org/10.3390/ma15134373.
I¸sıldar, A., van de Vossenberg, J., Rene, E.R., van Hullebusch, E.D., Lens, P.N., 2016. Two-step bioleaching of copper and gold from discarded printed circuit boards (PCB). Waste Manag. 57, 149–157. https://doi.org/10.1016/j.wasman.2015.11.033.
Ilyas, S., Anwar, M.A., Niazi, S., Ghauri, M.A., 2007. Bioleaching of metals from electronic scrap by moderately thermophilic acidophilic bacteria. Hydrometallurgy 88, 180–188. https://doi.org/10.1016/j.hydromet.2007.04.007.
Ilyas, S., Ruan, C., Bhatti, H.N., Ghauri, M.A., Anwar, M.A., 2010. Column bioleaching of metals from electronic scrap. Hydrometallurgy 101, 135–140. https://doi.org/10.1016/j.hydromet.2009.12.007.
Is¸ildar, A., Rene, E.R., van Hullebusch, E.D., Lens, P.N.L., 2018. Electronic waste as a secondary source of critical metals: management and recovery technologies. Resour. Conserv. Recycl. 135, 296–312. https://doi.org/10.1016/j.resconrec.2017.07.031.
Ivanus, R.C., 2010. Bioleaching of metals from electronic scrap by pure and mixed culture of Acidithiobacillus ferrooxidans and Acidithiobacillus thiooxidans. Metal. Int. 15 (4), 62–70.
Kang, K.D., Ilankoon, I.M.S.K., Dushyantha, N., Chong, M.N., 2021. Assessment of pre-treatment techniques for coarse printed circuit boards (PCBs) recycling. Miner. 10, 1134. https://doi.org/10.3390/min11101134.
Kaya, M., 2016. Recovery of metals and nonmetals from electronic waste by physical and chemical recycling processes. Waste Manag. 57, 64–90. https://doi.org/10.1016/j.wasman.2016.08.004.
Khanna, R., Saini, R., Park, M., Ellamparuthy, G., Biswal, S.K., Mukherjee, P.S., 2020. Factors influencing the release of potentially toxic elements (PTEs) during thermal processing of electronic waste. Waste Manag. 105, 414–424. https://doi.org/10.1016/j.wasman.2020.02.026.
Korf, N., Løvik, A.N., Figi, R., Schreiner, C., Kuntz, C., Mählitz, P.M., Rösslein, M., Wäger, P., Rotter, V.S., 2019. Multi-element chemical analysis of printed circuit boards – challenges and pitfalls. Waste Manag. 92, 124–136. https://doi.org/10.1016/j.wasman.2019.04.061.
Koyanaka, S., Endoh, S., Ohya, H., 2006. Effect of impact velocity control on selective grinding of waste printed circuit boards. Adv. Powder Technol. 17, 113–126. https://doi.org/10.1163/156855206775123467.
Krishnan, S., Zulkapli, N.S., Kamyab, H., Taib, S.M., Din, M.F.B.M., Majid, Z.A., Chaiprapat, S., Kenzo, I., Ichikawa, Y., Nasrullah, M., Chelliapan, S., Othman, N., 2021. Current technologies for recovery of metals from industrial wastes: an overview. Environ. Technol. Innov. 22, 101525 https://doi.org/10.1016/j.eti.2021.101525.
Kumar, A., Holuszko, M., Espinosa, D.C.R., 2017. E-waste: an overview on generation, collection, legislation and recycling practices. Resour. Conserv. Recycl. 122, 32–42. https://doi.org/10.1016/j.resconrec.2017.01.018.
Kumar, A., Holuszko, M.E., Janke, T., 2021. Analysis of rejects from waste printed circuit board processing as an alternative fuel for the cement industry. Waste Manag. Res. J. Sustain. Circ. Econ. 39, 841–848. https://doi.org/10.1177/0734242X20952847.
Liang, G., Tang, J., Liu, W., Zhou, Q., 2013. Optimizing mixed culture of two acidophiles to improve copper recovery from printed circuit boards (PCBs). J. Hazard. Mater. 250–251, 238–245. https://doi.org/10.1016/j.jhazmat.2013.01.077.
Lucchesi, C.A., Hirn, C.F., 1960. EDTA titration of total Iron in Iron(II) and Iron(III) mixtures. Application to Iron driers. Anal. Chem. 32, 1191–1193.
Mahmoud, A., Cezac, P., Hoadley, A.F., Contamine, F., D'hugues, P., 2017. A review of sulfide minerals microbially assisted leaching in stirred tank reactors. Int. Biodeterior. Biodegrad. 119, 118–146. https://doi.org/10.1016/j.ibiod.2016.09.015.
Mir, S., Dhawan, N., 2022. A comprehensive review on the recycling of discarded printed circuit boards for resource recovery. Resour. Conserv. Recycl. 178, 106027 https://doi.org/10.1016/j.resconrec.2021.106027.
Mishra, D., Kim, D.J., Ralph, D.E., Ahn, J.G., Rhee, Y.H., 2008. Bioleaching of metals from spent lithium ion secondary batteries using Acidithiobacillus ferrooxidans. Waste Manag. 28, 333–338. https://doi.org/10.1016/j.wasman.2007.01.010.
Modin, O., Fuad, N., Rauch, S., 2017. Microbial electrochemical recovery of zinc. Electrochim. Acta 248, 58–63. https://doi.org/10.1016/j.electacta.2017.07.120.
Moyo, T., Chirume, B.H., Petersen, J., 2020. Assessing alternative pre-treatment methods to promote metal recovery in the leaching of printed circuit boards. Resour. Conserv. Recycl. 152 https://doi.org/10.1016/j.resconrec.2019.104545.
Murugesan, M.P., Kannan, K., Selvaganapathy, T., 2020. Bioleaching recovery of copper from printed circuit boards and optimization of various parameters using response surface methodology (RSM). Mater. Today Proc. 26 (2), 2720–2728. https://doi.org/10.1016/j.matpr.2020.02.571.
Naseri, T., Mousavi, S.M., 2022. Insights into the polysaccharides and proteins production from Penicillium citrinum during bioleaching of spent coin cells. Int. J. Biol. Macromol. https://doi.org/10.1016/j.ijbiomac.2022.04.042.
Naseri, T., Beigi, V., Namdar, A., Keikavousi Behbahan, A., Mousavi, S.M., 2022a. Biohydrometallurgical recycling approaches for returning valuable metals to the battery production cycle. In: Nano Technology for Battery Recycling, Remanufacturing, and Reusing. Elsevier, pp. 217–246. https://doi.org/10.1016/B978-0-323-91134-4.00005-4.
Naseri, T., Pourhossein, F., Mousavi, S.M., Kaksonen, A.H., Kuchta, K., 2022b. Manganese bioleaching: an emerging approach for manganese recovery from spent batteries. Rev. Environ. Sci. Biotechnol. 21, 447–468. https://doi.org/10.1007/s11157-022-09620-5.
Otsuki, A., Gonçalves, P.P., Leroy, E., 2019a. Selective milling and elemental assay of printed circuit board particles for their recycling purpose. Metals 9, 899. https://doi.org/10.3390/met9080899.
Otsuki, A., Gonçalves, P.P., Stieghorst, C., Révay, Z., 2019b. Non-destructive characterization of mechanically processed waste printed circuit boards: X-ray fluorescence spectroscopy and prompt gamma activation analysis. J. Compos. Sci. 3, 54. https://doi.org/10.3390/jcs3020054.
Otsuki, A., La Mensbruge, L.D., King, A., Serranti, S., Fiore, L., Bonifazi, G., 2020. Nondestructive characterization of mechanically processed waste printed circuit boards - particle liberation analysis. Waste Manag. 102, 510–519. https://doi.org/10.1016/j.wasman.2019.11.006.
Park, S., Kim, S., Han, S., Kim, B., Kim, B., Han, Y., Park, J., 2018. Liberation characteristics assessment for copper component in PCB comminution product by image analysis. Mater. Trans. 59 (9), 1493–1500. https://doi.org/10.2320/matertrans.M2018113.
Pokhrel, P., Lin, S.-L., Tsai, C.-T., 2020. Environmental and economic performance analysis of recycling waste printed circuit boards using life cycle assessment. J. Environ. Manag. 276, 111276 https://doi.org/10.1016/j.jenvman.2020.111276.
Pourhossein, F., Mousavi, S.M., 2018. Enhancement of copper, nickel, and gallium recovery from LED waste by adaptation of Acidithiobacillus ferrooxidans. Waste Manag. 79, 98–108.
Qiu, Ruijun, Lin, M., Ruan, J., Fu, Y., Hu, J., Deng, M., Tang, Y., Qiu, Rongliang, 2020. Recovering full metallic resources from waste printed circuit boards: a refined review. J. Clean. Prod. 244, 118690 https://doi.org/10.1016/j.jclepro.2019.118690.
Rao, M.D., Singh, K.K., Morrison, C.A., Love, J.B., 2020. Challenges and opportunities in the recovery of gold from electronic waste. RSC Adv. 10, 4300–4309. https://doi.org/10.1039/c9ra07607g.
Robinson, B.H., 2009. E-waste: an assessment of global production and environmental impacts. Sci. Total Environ. 408, 183–191. https://doi.org/10.1016/j.scitotenv.2009.09.044.
Sahan, M., Kucuker, M., Demirel, B., Kuchta, K., Hursthouse, A., 2019. Determination of metal content of waste mobile phones and estimation of their recovery potential in Turkey. Int. J. Environ. Res. Public Health 16, 887. https://doi.org/10.3390/ijerph16050887.
Sethurajan, M., van Hullebusch, E.D., Fontana, D., Akcil, A., Deveci, H., Batinic, B., Leal, J.P., Gasche, T.A., Ali Kucuker, M., Kuchta, K., Neto, I.F.F., Soares, H.M.V.M., Chmielarz, A., 2019. Recent advances on hydrometallurgical recovery of critical and precious elements from end of life electronic wastes - a review. Crit. Rev. Environ. Sci. Technol. 49, 212–275. https://doi.org/10.1080/10643389.2018.1540760.
Sodha, A.B., Shah, M.B., Qureshi, S.A., Tipre, D.R., Dave, S.R., 2019. Decouple and compare the role of abiotic factors and developed iron and sulfur oxidizers for enhanced extraction of metals from television printed circuit boards. Sep. Sci. Technol. 54, 4. https://doi.org/10.1080/01496395.2018.1512616.
Sodha, A.B., Tipre, D.R., Dave, S.R., 2020. Optimisation of biohydrometallurgical batch reactor process for copper extraction and recovery from non-pulverized waste printed circuit boards. Hydrometallurgy 191, 105170. https://doi.org/10.1016/j.hydromet.2019.105170.
Syed, S., 2012. Recovery of gold from secondary sources-a review. Hydrometallurgy 115–116, 30–51. https://doi.org/10.1016/j.hydromet.2011.12.012.
Tabelin, C.B., Park, I., Phengsaart, T., Jeon, S., et al., 2021. Copper and critical metals production from porphyry ores and E-wastes: a review of resource availability, processing/recycling challenges, socio-environmental aspects, and sustainability

issues. Resour. Conserv. Recycl. 170, 105610 https://doi.org/10.1016/j.resconrec.2021.105610.
Tapia, J., Dueñas, A., Cheje, N., Soclle, G., Patiño, N., Ancalla, W., Tenorio, S., Denos, J., Taco, H., Cao, W., et al., 2022. Bioleaching of heavy metals from printed circuit boards with an acidophilic Iron-oxidizing microbial consortium in stirred tank reactors. Bioengineering 9, 79. https://doi.org/10.3390/bioengineering 9020079.
Tiwary, C.S., Kishore, S., Vasireddi, R., Mahapatra, D.R., Ajayan, P.M., Chattopadhyay, K., 2017. Electronic waste recycling via cryo-milling and nanoparticle beneficiation. Mater. Today 20, 67–73. https://doi.org/10.1016/j.mattod.2017.01.015.
Touze, S., Guignot, S., Hubau, A., Devau, N., Chapron, S., 2020. Sampling waste printed circuit boards: achieving the right combination between particle size and sample mass to measure metal content. Waste Manag. 118, 380–390. https://doi.org/10.1016/j.wasman.2020.08.054.
Tuncuk, A., Stazi, V., Akcil, A., Yazici, E.Y., Deveci, H., 2012. Aqueous metal recovery techniques from e-scrap: hydrometallurgy in recycling. Miner. Eng. 25, 28–37. https://doi.org/10.1016/j.mineng.2011.09.019.
Ueda, T., Oki, T., Koyanaka, S., 2017. Effect of particle shape on the stereological Bias of the degree of liberation of Biphase particle systems. Mater. Trans. 58, 280–286. https://doi.org/10.2320/matertrans.M-M2016837.
Valix, M., Usai, F., Malik, R., 2001. The electro-sorption properties of nickel on laterite gangue leached with an organic chelating acid. Miner. Eng. 14, 205–215. https://doi.org/10.1016/S0892-6875(00)00176-X.
Vardanyan, A., Stepanyan, S., Vardanyan, N., Markosyan, L., Sand, W., Vera, M., Zhang, R., 2015. Study and assessment of microbial communities in natural and commercial bioleaching systems. Miner. Eng. 81, 167–172. https://doi.org/10.1016/j.mineng.2015.05.001.
Vardanyan, A., Vardanyan, N., Aâtach, M., Malavasi, P., Gaydardzhiev, S., 2022a. Bio-assisted leaching of non-ferrous metals from waste printed circuit boards—importance of process parameters. Metals 12, 2092. https://doi.org/10.3390/met12122092.
Vardanyan, A., Vardanyan, N., Abrahamyan, N., Aatach, M., Gaydardzhiev, S., 2022b. Sequential biologically assisted extraction of cu and Zn from printed circuit boards (PCB). Int. J. Environ. Stud. https://doi.org/10.1080/00207233.2022.2126122.
Verma, H.R., Singh, K.K., Mankhand, T.R., 2017. Comparative study of printed circuit board recycling by cracking of internal layers using organic solvents dimethylformamide and dimethylacetamide. J. Clean. Prod. 142, 1721–1727. https://doi.org/10.1016/j.jclepro.2016.11.118.
Vermeșan, H., Tiuc, A.-E., Purcar, M., 2019. Advanced recovery techniques for waste materials from IT and telecommunication equipment printed circuit boards. Sustainability 12, 74. https://doi.org/10.3390/su12010074.
Vidyadhar, A., Das, A., 2013. Enrichment implication of froth flotation kinetics in the separation and recovery of metal values from printed circuit boards. Sep. Purif. Technol. 118, 305–312. https://doi.org/10.1016/j.seppur.2013.07.027.
Wang, L., He, J., Xia, A., Cheng, M., Yang, Q., Du, C., Wei, H., Huang, X., Zhou, Q., 2017a. Toxic effects of environmental rare earth elements on delayed outward potassium channels and their mechanisms from a microscopic perspective. Chemosphere 181, 690–698. https://doi.org/10.1016/j.chemosphere.2017.04.141.
Wang, H., Zhang, S., Li, B., Pan, D., Wu, Y., Zuo, T., 2017b. Recovery of waste printed circuit boards through pyrometallurgical processing: a review. Resour. Conserv. Recycl. 126, 209–218. https://doi.org/10.1016/j.resconrec.2017.08.001.
Wills, B., Finch, J.A., 2016. Wills' mineral processing technology: An introduction to the practical aspects of ore treatment and mineral recovery. In: Butterworth-Heinemann. Elsevier, Amsterdam, The Netherlands.
Xia, M.C., Wang, Y.P., Peng, T.J., Shen, L., Yu, R.L., Liu, Y.D., Chen, M., Li, J.K., Wu, X.L., Zeng, W.M., 2017. Recycling of metals from pretreated waste printed circuit boards effectively. J. Biosci. Bioeng. 123, 714–721. https://doi.org/10.1016/j.jbiosc.2016.12.017.
Xolo, L., Moleko-Boyce, P., Makelane, H., Faleni, N., Tshentu, Z., 2021. Status of recovery of strategic metals from spent secondary products. Minerals 11, 673. https://doi.org/10.3390/min11070673.
Yang, C., Zhu, N., Shen, W., Zhang, T., Wu, P., 2017. Bioleaching of copper from metal concentrates of waste printed circuit boards by a newly isolated Acidithiobacillus ferrooxidans strain Z1. J. Mater. Cycles Waste Manag. 19, 247–255. https://doi.org/10.1007/s10163-015-0414-7.
Yken, J.V., Cheng, K.Y., Boxall, N.J., Nikoloski, A.N., Moheimani, N., Valix, M., Sahajwalla, V., Kaksonen, A.H., 2020. Potential of metals leaching from printed circuit boards with biological and chemical lixiviants. Hydrometallurgy 196, 105433. https://doi.org/10.1016/j.hydromet.2020.105433.
Zhang, S., Forssberg, E., 1999. Intelligent liberation and classification of electronic scrap. Powder Technol. 105, 295–301. https://doi.org/10.1016/S0032-5910(99)00151-5.
Zhou, Y., Qiu, K., 2010. A new technology for recycling materials from waste printed circuit boards. J. Hazard. Mater. 175, 823–828. https://doi.org/10.1016/j.jhazmat.2009.10.083.
Zhou, H.-B., Zeng, W.-M., Yang, Z.-F., Xie, Y.-J., Qiu, G.-Z., 2009. Bioleaching of chalcopyrite concentrate by a moderately thermophilic culture in a stirred tank reactor. Bioresour. Technol. 100, 515–520. https://doi.org/10.1016/j.eti.2021.101525.
Zhou, X., Guo, J., Lin, K., Huang, K., Deng, J., 2013. Leaching characteristics of heavy metals and brominated flame retardants from waste printed circuit boards. J. Hazard. Mater. 246-247, 96–102. https://doi.org/10.1016/j.jhazmat.2012.11.065.
Zhu, N., Xiang, Y., Zhang, T., Wu, P., Danga, Z., Li, P., Wu, J., 2011. Bioleaching of metal concentrates of waste printed circuit boards by mixed culture of acidophilic bacteria. J. Hazard. Mater. 192, 614–619. https://doi.org/10.1016/j.jhazmat.2011.05.062.